Revista Mexicana de Física
ISSN: 0035-001X
rmf@ciencias.unam.mx
Sociedad Mexicana de Física A.C.
México

Miranda, A.; Guzmán, D.; Pérez-Meana, H.M.; Cruz-Irisson, M.
Semiempirical supercell approach to calculate the electronic and optical properties of Si quantum wires
Revista Mexicana de Física, vol. 53, núm. 7, diciembre, 2007, pp. 220-2224
Sociedad Mexicana de Física A.C.
Distrito Federal, México

Semiempirical supercell approach to calculate the electronic and optical properties of Si quantum wires

A. Miranda, D. Guzmán, H.M. Peréz-Meana, and M. Cruz-Irisson
Instituto Politécnico Nacional
Sección de Estudios de Posgrado e Investigación, ESIME-Culhuacan,
Av. Santa Ana 1000, 04430 México, D.F.
e-mail: amirandad9700@ipn.mx

Recibido el 30 de noviembre de 2006; aceptado el 8 de octubre de 2007

Energy band gap and optical absorption of [001] oriented Si nanowires with diverse square cross-sections are calculated by using the sp^3s^* semi-empirical tight-binding (TB) model with a supercell approach. Each surface dangling bond is saturated with a hydrogen atom. The results of the variation band gap are compared with those obtained by TB-$sp^3d^5s^*$, the density functional theory, and experimental data in agreement with the quantum confinement scheme. The imaginary part of the dielectric function is calculated by using the interconnected and free standing (without interconnection) models for the Si skeleton. This microscopic supercell model predicts the low frequency tail in the absorption spectrum, which appears even without the allowance for the indirect optical transitions.

Keywords: Nanostructures; silicon; tight-binding.

Se calculan, por medio de una aproximación semi-empírica de amarre-fuerte sp^3s^* aplicada a un modelo de superceldas, la brecha de energía y la absorción óptica de nanoalambres de Si orientados en la dirección [001] de sección transversal cuadrada de diferentes tamaños. Cada enlace suelto de la superficie es saturado con un átomo de hidrógeno. Los resultados de la variación de la brecha de energía son comparados con los obtenidos por TB-$sp^3d^5s^*$, teoría de funcionales de la densidad, y con datos experimentales acordes con el esquema de confinamiento cuántico. La parte imaginaria de la función dieléctrica es calculada usando modelos con interconexión y sin interconexión para el esqueleto de Si. Estos modelos de superceldas microscópicos predicen una cola a baja frecuencia en el espectro de absorción, la cual aparece aun sin la consideración de transiciones ópticas indirectas.

Descriptores: Nanoestructuras; silicio; amarre-fuerte.

PACS: 73.21.Hb; 78.67.Lt; 78.67.-n

1. Introduction

From the theoretical point of view, there are many approaches which allow the research of the electronic and optical properties of nanostructured crystals. The *ab-initio* method has been extensively used due to the possibility of a fully atomistic description of these materials [1, 2]. They have become very efficient thanks to the continuously increasing computer performance and algorithm speed. On the other hand, semiempirical methods remain a vigorous tool [3], giving the opportunity to simulate real nanocrystals, made of tens of thousands of atoms with diameters of several nanometers. The properties of large nanocrystals are both qualitatively and quantitatively described within such approaches, provided that the transferability of the parameters from the bulk to the nanoscale is an acceptable approximation.

Since the early work of Vogl *et al*. [4], semi-empirical tight-binding methods have been used to investigate the electronic structure of semiconductors. In spite of their mathematical simplicity, the one electron approach can be very useful to explain qualitative features, basic mechanisms of interaction and their connection to the observed band structure, chemical trends, etc. [5].

Semi-empirical Hamiltonian depends on empirical parameters. It is believed that once a good, robust set of parameters is determined, which satisfactorily reproduces the band structure of the bulk, reliable and useful insight can be gained in the study of the more complex systems, like the interconnections of Si nanowires (SiNWs) in porous silicon (por-Si).

It was soon realized [4] that a basis set which contains only valence atomic orbitals is not suitable to describe the conduction bands of semiconductors. This comes from the well known inadequacy of molecular orbital methods to represent empty electronic levels. However, it has been possible to cope with this limitation by including, in the basis set, excited s orbitals (s^*). This has led to a considerable improvement of results, in particular, of the description of the indirect gap appearing in most semiconductors of the zincblende structure [4].

On the other hand, great interest has been devoted in the last years to the study of the electronic and optical properties of SiNWs and por-Si. Despite the large number of papers that have been published on this subject, there are still some aspects which are controversial and not fully understood. Just to give a few examples, we can mention the Stokes shift between the absorption gap and the photoluminescence peak [6], the annihilation of the oscillator strength [7], the origin of the luminescence, the role of excitons and surface states [8].

Reducing the size pushes toward the approach of the *full quantum limit*, where the properties of the nanowire are sub-

stantially different from the bulk material. For this reason, a detailed knowledge of such system is extremely interesting both from the fundamental physics standpoint and for what concerns the molecular electronic applications because the size of the device is being continuously reduced; 10 nm thick SiNWs can now be routinely grown.

In this paper we consider a semiempirical tight-binding (TB) approach, based on a set of localized wave function (sp^3s^*) that is very efficient in the study of large structures [9]. We have adopted wire geometry with a bulk-like structure in the interior, as observed in experiments [10, 11], and carried out the calculations using two types of structures: isolated quantum wires and interconnected Si skeleton, like por-Si.

2. Electronic structure

We present here the electronic band structure for Si nanowires, oriented along the [001] direction, calculated using a sp^3s^* TB Hamiltonian. We construct all of the nanowires with a square cross-section [12]. Their side and top views are shown in Fig. 1. As an idealization, it is assumed that there is no relaxation of the bulk lattice. The hydrogenation of semiconductor surfaces has many important aspects. Hydrogen modifies both the chemical reactivity and the electrical conductivity of the surfaces on which it is adsorbed. Hydrogen surfaces are passivated, that is, they are less reactive compared to the clean surfaces. We suppose that the nanostructures have the same lattice structure and the same interatomic distance as bulk Si, and that all the dangling bonds are saturated with hydrogen atoms described by $1s$ orbital. For simplicity, we also suppose that there is no hydrogen-hydrogen interaction. These atoms are used to simulate the bonds at the surface of the wire and sweep surface states out of the energy band gaps. We assume that the H-saturated dangling bonds on the surface of the wire have the natural H-Si bond length. We are aware that we are simplifying enormously the surface description, ignoring other possible saturators and surface reconstruction. Clearly, this description is insufficient to study photoluminescence phenomena. This approach, though missing surface reconstruction effects, has already proved to be highly successful in describing intrinsic quantum confinement in semiconductor nanocrystals [1]. We use a supercell method in which the basic unit cell has translational symmetry in the z axis, with a period equal to lattice constant *a*. The principle of the TB method is to expand the quasiparticles wave function onto a basis of atomic orbitals. The TB parameters for Si-Si are taken from [4]. The Si-H TB parameters were calculated from fits to SiH_4 molecules, with the bond lengths taken to be 1.48 Å [9].

The calculations of quantum wire electronic properties have been performed in the one-dimensional Brillouin zone, $[-\pi/a, \pi/a]$, along the wire axis. The calculated band structure and density of states around band gap are shown in Fig. 2 for a SiNW of 32 Si-atoms supercell. Notice the shift of the conduction-band minimum (arrow) towards the center of the Brillouin zone (BZ) with respect to the bulk crystalline Si (c-Si) case. Also, notice a clear broadening of the band gap due to quantum confinement, and the cleaning of the gap due to hydrogen surface passivation.

It is also important to notice that dangling bond-like states do not appear within the band gap zone for all SiNWs. This is an indication of hydrogen saturation of the dangling bonds that provides a smooth termination of the orbitals, similar to a boundary condition at the interface with a wide-gap material.

The thickness effect on the band gaps of quantum wires is studied by considering eight wire widths ($\sim$ 0.5 - 4nm) in a systematic manner. The features of the bands in all cases are similar because they are oriented along the same direction. The profile of the band dispersion does not change when the diameter is decreased. Nevertheless, the valence band with the maximum energy gets pushed down, and this makes the thinner quantum wire have an almost direct band gap. The

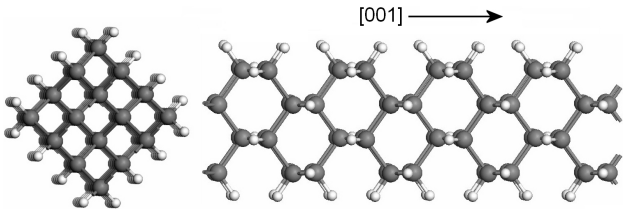

FIGURE 1. Ball and stick model of silicon nanowire along the [001] directions, viewed from the top (left) and the side (right).

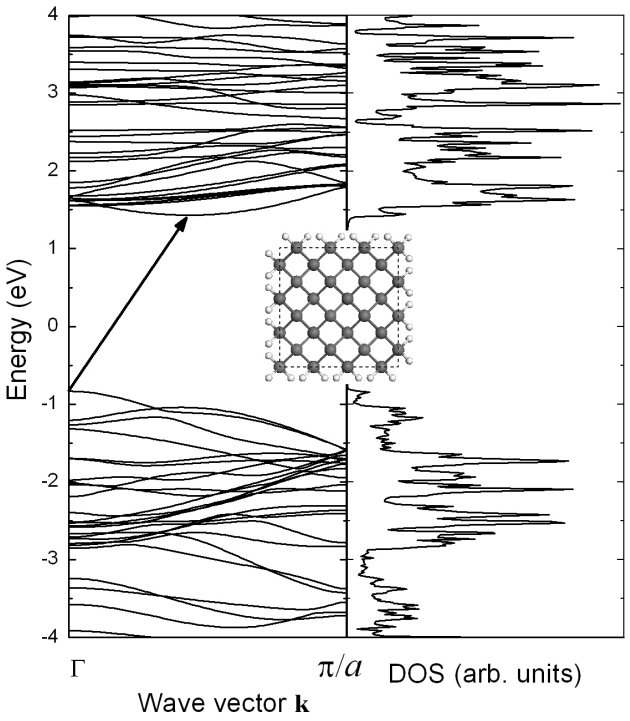

FIGURE 2. One-dimensional band dispersion for [001]-oriented silicon quantum wire (*d*=1.08 nm) with -H termination. The arrow shows the indirect gap.

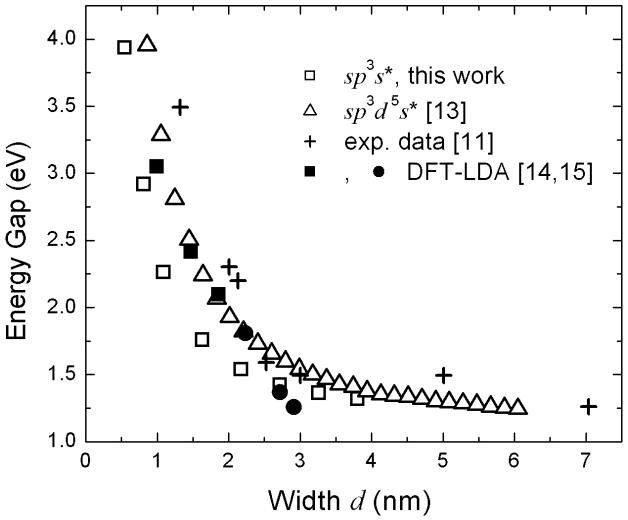

FIGURE 3. Energy band gap comparison among TB sp^3s^* calculations (our results □) , $sp^3d^5s^*$ (△, Ref. 13), DFT-LDA (■, •, Refs. 14 and 15), and experimental data (+, [11]).

band gap of the nanowires increases monotonically with decreasing thickness (Fig. 3), as has also been found in previous studies [11, 13–15]. This is due to the quantum confinement of the carriers, which is particularly strong in the range of widths we have studied. These results show that it could be possible to prepare SiNWs with desired band gaps by varying the thickness and by performing band gap engineering.

To evaluate the accuracy and efficiency of the TB-sp^3s^* method, it is necessary to compare this work with results of other methods and experimental data. In Fig. 3, we compare our numerical results, sp^3s^*-TB calculation (□), with: $sp^3d^5s^*$ (△), DFT-LDA (■, •), and measured band gap [11] for Si quantum wires along the [112] direction (+). Since this direction is very different to the [001] direction used in our theoretical model (□), this comparison should be viewed with caution. However, despite the fact that our model is very simple, it gives a good qualitative agreement with those obtained by experimental data [11] according with the quantum confinement scheme.

3. Optical properties

Having established a TB model which successfully accounts for the band structure of SiNWs, we proceed with the computation of the optical properties of the isolated and interconnected SiNWs. For the calculation of the imaginary part $\varepsilon_2(\omega)$ of the dielectric function, we use the expression

$$\varepsilon_2(\omega) = \frac{2e^2\pi}{\Omega\varepsilon_0} \sum_{\mathbf{k},v,c} |\langle c,\mathbf{k}|\hat{\mathbf{e}}\cdot\mathbf{r}|v,\mathbf{k}\rangle|^2 \times \delta\left(E^c_{\mathbf{k}} - E^v_{\mathbf{k}} - \hbar\omega\right), \quad (1)$$

where $|v,\mathbf{k}\rangle$ and $|c,\mathbf{k}\rangle$ are valence and conduction band Bloch states with energies $E^v_{\mathbf{k}}$ and $E^c_{\mathbf{k}}$, respectively, $\mathbf{r}$ is the electron position, and $\hat{\mathbf{e}}$ is the polarization of light. In the TB scheme, the Bloch functions over the local Si orbitals $|\mathbf{R}j\mu\rangle$ can be written as

$$|v,\mathbf{k}\rangle = \frac{1}{\sqrt{N}} \sum_{\mathbf{R}} e^{i\mathbf{k}\cdot\mathbf{R}} \sum_{\mu j} A^v_{j\mu}(\mathbf{k})|\mathbf{R}j\mu\rangle. \quad (2)$$

Here $\mathbf{R}$ are the Bravais vectors giving the positions of the supercells, j enumerates Si atoms within the supercell, $\mu = s$, p_x, p_y, p_z, s^* identifies the orbital, and N is the total number of supercells. Thus, it is necessary to know the position of matrix elements between the atomic orbitals.

There are two approaches in the literature to evaluate $(\mathbf{R}'j'\lambda'|\mathbf{r}|\mathbf{R}j\mu)$. One approach uses inter-atomic dipole matrix elements, while the other approach uses intra-atomic dipole matrix elements [16]. In both cases, if the overlapping of orbitals belonging to different atoms is small, one can neglect the interatomic dipole matrix elements. Between the orbitals belonging to the same Si atoms ($\mathbf{R} = \mathbf{R}'$ and $j = j'$), one has

$$(\mathbf{R}j\lambda|\mathbf{r}|\mathbf{R}j\mu) = (\mathbf{R} + \mathbf{u}_j)\delta_{\lambda\mu} + d_{\lambda\mu}, \quad (3)$$

where $\mathbf{u}_j$ gives the position of the jth atom in the supercell, and $d_{\lambda\mu}$ is the intra-atomic matrix element, which is dependent on $\mathbf{R}$, and j is nonzero only for $\mu \neq \lambda$. Within the interatomic approach, the polarizability of a free atom is considered to be much smaller than that of the corresponding semiconductor, and only the first term of Eq. (3) is considered. In contrast, the second approach (intra-atomic) considers the contribution to the dipole matrix element coming from different orbitals at the same atom, without neglecting the first term in Eq. (3). For Si, the nonzero matrix elements $d_{\lambda\mu}$ in Eq. (3) are $(s|x|p_x) = 0.27$ Å and $(s^*|x|p_x) = 1.08$ Å. In our calculations of the dielectric function we allowed for both contributions [16]. The real part of the dielectric function could be obtained by the Kramers-Kroning analysis. The calculations have been carried out for light polarized in the [100] direction, *i.e.*, perpendicular to the wire alignment.

In some nanostructured materials, such as in por-Si nanostructures, its skeleton constituting a network can be represented by interconnected Si nanoparticles. Such interconnection could be important in electronic states, optical properties, and electrical transport in a single nanowire or in a whole nanowire network.

The imaginary part of the dielectric function obtained for the isolated Si Nanowire (without interconnection) is shown in Fig. 4. For this case, the interconnectivity of the silicon skeleton is lost; the energy spectrum is characterized by very flat minibands, and some of them do not possess dispersion at all. It results in the appearance of a lot of peaks in the absorption spectrum. Figure 5 shows the frequency dependence of ε_2 calculated for the interconnected case (por-Si) of a 32-atom supercell with a fourteen-atom columnar pore (43.75% porosity). This 32-atom supercell is built by joining four cubes of side $a = 5.43$Å in the XY plane, leading to a tetragonal structure with parameters $A = 2a$, $B = 2a$ and $C = a$. Periodic boundary conditions are considered in the

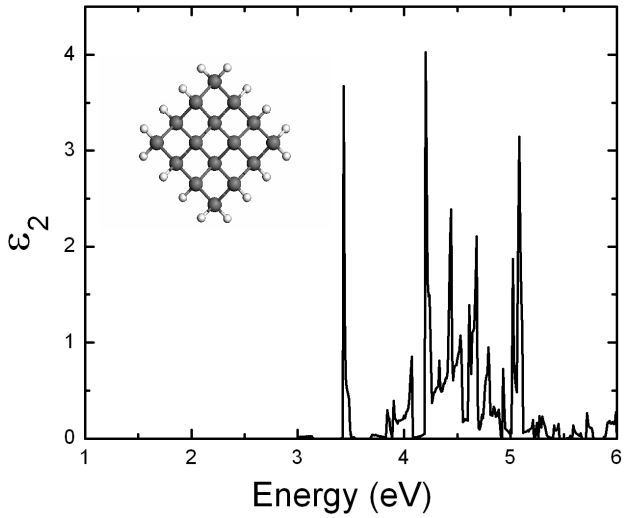

FIGURE 4. The imaginary part of the dielectric function calculated from an isolated Si nanowire 16-atom supercell (inset).

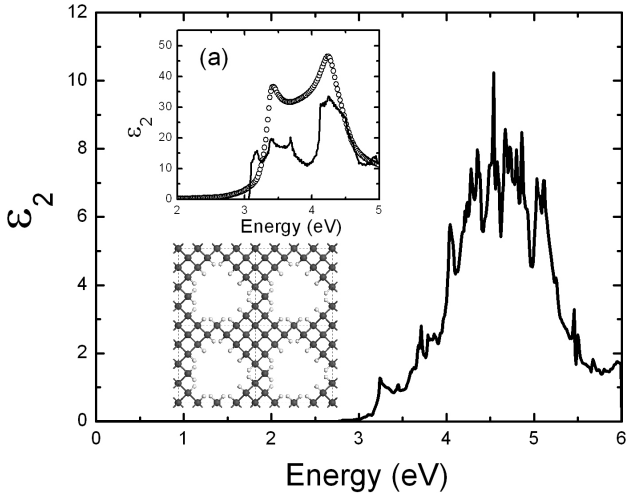

FIGURE 5. The imaginary part of the dielectric function, ε_2, calculated from an interconnected Si nanowires (por-Si). Inset: four 32-atom supercells with 14 Si atoms removed from each one (43.75% porosity). Fig. 5 (a) ε_2 as a function of photon energy for c-Si. The solid line represent our results obtained from TB, and the open circles represent the experimental data.

three directions. Since the supercells are XY plane extended, removing one atom in such supercells produces one-atom columnar pores along the Z-direction, and these columns form a square lattice on the XY plane. The inset of Fig. 5a represents a comparison between the calculated (solid line) dielectric function and the experimental data (open circles) [17] for the crystalline case (no pores). It is seen that the theory gives reasonably well the shape of the edge of the optical spectrum, in spite that no d-orbitals are considered. The position of the low energy peak and its intensity are underestimated. This can be attributed to the limits of the sp^3s^* first-neighbor TB parametrization, which fails to describe correctly the dispersion of the second conduction band. Notice that the dependence of the dielectric function on the frequency of the light is smoother for the interconnected case.

The interesting feature seen in Fig. 5 is the appearance of the low-frequency tail (between 2.0 and 3.0 eV) on the dielectric function of the por-Si. The direct optical absorption (without phonon assistance) is absent in this region in the c-Si case. This tail is the consequence of the umklapp processes, $\mathbf{k}_c - \mathbf{k}_v = \mathbf{G}$, where $\mathbf{G}$ is a reciprocal lattice vector of the lattice of pores. These transitions in c-Si are forbidden since they involve a big change of the momentum. After introducing the pores, the supercell becomes the *primitive cell* for the material, and these transitions can be thought as vertical transitions in the reduced BZ. The absorption coefficient could give interesting information on the nature of the band edge in a por-Si sample. It is worth mentioning, up to our knowledge, that we have found no experimental data for ε_2 in the literature for the porosity of 56.25% considered here.

4. Conclusions

In summary, we have studied, from semi-empirical tight binding approximation, the structures of free standing silicon nanowires oriented in the [001] direction and their electronic properties as a function of their widths. These properties are strongly influenced by quantum confinement. Despite the fact that our model is very simple, it gives a good qualitative agreement with experimental data. The loss of interconnectivity in the Si skeleton results in the appearance of a series of spikes in the optical spectrum due to the flattening of the energy subbands. In fact, the dielectric response in the isolated quantum wires is similar to the isolated quantum dots with discrete energy levels. The microscopic supercell model predicts the low-frequency tail in the optical response, which appears even without the allowance for the indirect (phonon-assisted) optical transitions. This tail is the consequence of the interplay between the umklapp optical absorption and the partial quantum confinement, as it was discussed in detail in Ref. 16. The interconection between the skeleton of porous silicon wires could be less important for the optical absorption than it should be expected for the transport properties of this material.

Acknowledgements

This work has been supported by projects SIP-IPN: 20070455 and CONACyT 49715-F. The computing facilities of DGSCA-UNAM are fully acknowledged.

1. M. Nolan, S. O'Callaghan, G. Fagas, and J.C. Greer, *Nano Lett.* **7** (2007) 34.
2. D.B. Migas, *J. Appl. Phys.* **98** (2005) 054310.
3. Y.M. Niquet, C. Delerue, G. Allan, and M. Lannoo, *Phys. Rev. B* **62** (2000) 5109.
4. P. Vogl, H.P. Hjalmarson and J.D. Dow, *J. Phys. Chem. Solids* **44** (1983) 365.
5. M. Murayama and T. Nakayama, *Phys. Rev. B* **49** (1994) 4710.
6. E. Degoli *et al.*, *Phys. Rev. B* **69** (2004) 155411.
7. I.Vasiliev, S. Öğüt, and J.R. Chelikowsky, *Phys. Rev. Lett.* **86** (2001) 1813.
8. M.V. Wolkin, J. Jorne, P.M. Fauchet, G. Allan, and C. Delerue, *Phys. Rev. Lett.* **82** (1999) 197.
9. M. Cruz, C. Wang, M.R. Beltrán, and J. Tagüeña-Martínez, *Phys. Rev. B* **53** (1996) 3827.
10. Y. Cui, L.J. Lauhon, M.S. Gudiksen, J. Wang, and C.M. Lieber, *Appl. Phys. Lett.* **78** (2001) 2214.
11. D.D.D. Ma, C.S. Lee, F.C.K. Au, S.Y. Tong, and S.T. Lee, *Science* **299** (2003) 1874.
12. P. Alfaro, A. Miranda, A.E. Ramos, and M. Cruz-Irisson, *Braz. J. Phys*. **36** (2006) 375.
13. G. Xi-Meng, and Y. Zhi-Ping, *Chin. Phys. Lett.* **22** (2005) 2651.
14. A.J. Read *et al.*, *Phys. Rev. Lett.* **69** (1992) 1232.
15. H. Scheel, S. Reich, and C. Thomsen, *Phys. Stat. Sol. (b)* **242** (2005) 2474.
16. M. Cruz, M.R. Beltrán, C. Wang, J. Tagüeña-Martínez, and Y. G. Rubo, *Phys. Rev. B* **59** (1999) 15381.
17. D.E. Aspnes and A.A. Studna, *Phys. Rev. B* **27**(1983) 985.